Single-particle states in $^{149}_{66}Dy_{83}$ at high spin

M. Gupta,[1] Pragya Das,[2] S. B. Patel,[1] R. K. Bhowmik,[3] T. Werner,[4–6] and Y. A. Akovali[4]

[1]*Department of Physics, University of Bombay, Bombay 400 098, India*
[2]*Department of Physics, Indian Institute of Technology, Bombay 400 076, India*
[3]*Nuclear Science Centre, New Delhi 110 067, India*
[4]*Physics Division, Oak Ridge National Laboratory, Oak Ridge, Tennessee 37831*
[5]*Department of Physics and Astronomy, University of Tennessee, Knoxville, Tennessee 37996*
[6]*Institute of Theoretical Physics, Warsaw University, PL-00-681 Warsaw, Poland*

(Received 12 February 1996)

High-spin states have been populated in the nucleus ^{149}Dy using the ^{122}Sn(^{32}S, $5n$)^{149}Dy reaction at a beam energy of 163 MeV. The experimental level scheme has been extended to a spin of $\frac{61}{2}\hbar$, corresponding to an energy of about 12 MeV, and is adequately explained in the context of the shell model. Most of the levels are characterized by maximally aligned single-particle states with no evidence of collectivity. An alternate shell-model approach has been adopted to assign shell-model configurations. [S0556-2813(96)01609-3]

PACS number(s): 23.20.Lv, 21.60.Cs, 25.70.Gh, 27.60.+j

I. INTRODUCTION AND MOTIVATION

Nuclei in the neighborhood of the doubly closed-shell nucleus ^{146}Gd have been known to exhibit a wide variety of behaviors including superdeformation, as a result of the large number of valence nucleons. Up to spins of about $40\hbar$, it has been possible, for the most part, to interpret the structure of these nuclei in the context of the shell model [1] with residual interactions. States with large angular momentum observed in the neutron deficient $A\sim150$ nuclei that lie in the neighborhood of doubly closed shells appear to be primarily composed of the alignment of single-particle states. Thus high-spin states in ^{149}Dy are expected to arise mainly from the alignment of valence nucleons [2,3]. Since the level spacing due to rotation around a symmetry axis is statistical in nature, one may expect the presence of yrast traps.

The $N=83$ nucleus ^{149}Dy is interesting for many reasons. With $Z=66$, this nucleus has two protons and one neutron outside the closed ^{146}Gd core. All of these three valence particles could carry high angular momentum built upon the configurations $h_{11/2}$ for the protons and $f_{7/2}$, $h_{9/2}$, and $i_{13/2}$ for the neutrons. The decay scheme developed here confirms that high-spin states arise as a direct consequence of the realignment of these valence nucleons. Parallel cascades appear in the established level scheme at about a spin of $\frac{31}{2}\hbar$, which is expected as a result of core breaking. High-spin multiplets of the $\pi h_{11/2}^2$ type that are seen to exist in the $N=82$ core spectra [4] also appear here and low-lying three-particle isomers are visible. Finally, the pattern of levels that feed multiple maximally aligned valence configurations suggest the existence of yrast isomers, a common occurrence in this mass region. The presence of an unusually long-lived 510-ms isomer at an excitation energy of 2.661 MeV was first noted [4,5] and later confirmed [6], pointing to the possibility that a different core structure may exist at higher spins. Since no comparably long ''yrast trap'' at low energies has been reported in any of the $N=83$ isotones Gd, Sm, and Nd, this provided further motivation for populating high-spin states in the present study.

Finally, prior to the present experiment the nucleus ^{149}Dy was known up to an excitation energy of about 7.4 MeV [3,5,6], corresponding to a tentatively assigned spin of $\frac{49}{2}\hbar$ (which is, in fact, our $\frac{45}{2}^-\hbar$ state as shown in Fig. 1). Since all the earlier spin-parity assignments up to this level were uncertain, additional experimental data seemed to be necessary in order to determine a more reliable level structure. We have found that the two previously placed 451.7 keV and 248.4 keV transitions around $E_x\sim6.0$ MeV do not belong to this nucleus.

II. EXPERIMENTAL SETUP AND ANALYSIS

High-spin states in the nucleus ^{149}Dy were populated using the reaction ^{122}Sn(^{32}S, $5n$)^{149}Dy at a beam energy of 163 MeV using an enriched tin target of thickness 1.4 mg/cm^2 with a 25-mg/cm^2 lead backing. The relative production cross sections of the residues at this excitation energy were qualitatively consistent with those predicted by the statistical model code CASCADE. The ^{32}S beam was provided by the Nuclear Science Centre, New Delhi. Gamma-gamma coincidences were measured using the Gamma Detector Array (GDA), which consisted of seven 23% n-type Compton-suppressed HPGe detectors positioned at a distance of 180 mm from the target, along with a fourteen-element bismuth geminate (BGO) multiplicity filter. The anti-Compton shields (ACS's) were of a symmetric design consisting of NaI capped BGO crystals. Any direct radiation from the target onto the ACS's was guarded against by heavy metal (tantalum alloy) collimators of 30 mm placed between each detector and the target. The Compton-suppressed HPGe detectors were mounted so that three detectors were at an angle of 153°, with three more at 99° and with one at 45°, to the beam axis. The typical HPGe-ACS combination yielded a peak-to-total ratio of about 55% with a standard ^{60}Co source. The details of the experimental setup appear in earlier publications, for instance [7]. Since the multiplicity filter cov-

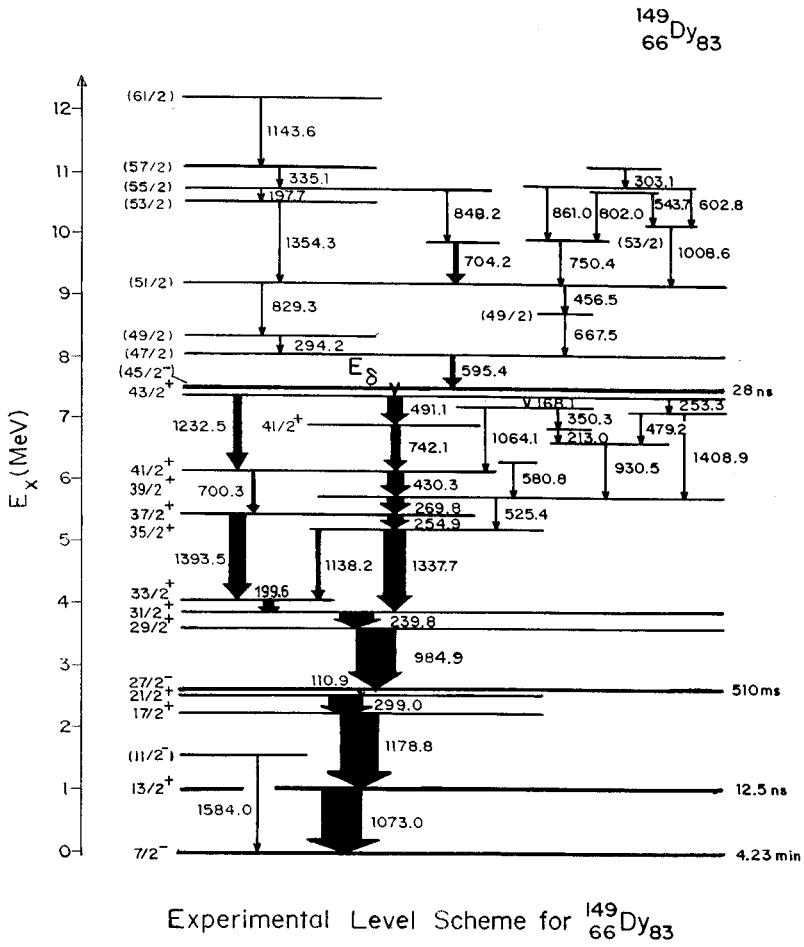

FIG. 1. Experimental level scheme deduced for the $N=83$ nucleus ^{149}Dy.

ered only about 35% of the total solid angle, multiplicity information has not been relied upon within the present analysis. About 8×10^7 multiparameter events were recorded in list mode. Only twofold or higher coincidences were stored and a zero-suppression algorithm was incorporated at the software level, thus preventing the recording of data originating from false triggering. The pulse heights in each detector were software gain matched and the data were sorted into a 1024×1024 total E_γ-E_γ matrix. Post-processing of background subtracted data was done by creating one-dimensional histograms for γ energies in one detector gated by a suitable transition in another detector. The coincidence time window was fixed at 40 ns. On account of this, the intensities of all of the transitions below the 510-ms isomer [4,5] have been severely attenuated when gating on the 985-keV transition. As such, the level scheme above an excitation energy of 2661 keV was developed independently of the region below. Furthermore, with regard to the five transitions below this isomeric state, we have adopted the multipolarities, spin assignments, and relative intensities as in [5,6] with the exception of the 1584 keV γ ray, which was placed in the scheme developed here. Figure 2 shows three coincidence spectra gated by the 985 keV, 595 keV, and 1394 keV transitions. The intensities of all the lines with an energy of under 250 keV were corrected for by their total electron conversion coefficients. The level scheme in Fig. 1 has been developed using the observed coincidence relationship, the directional correlation (DCO) ratios, and intensity arguments. Table I shows the transition energies, excitation energy, relative intensity (with the intensity of the 984.9 keV transition taken as 100%), DCO ratios, and spin-parity assignments for all the transitions placed in this study. The DCO ratios were arrived at by using γ-coincidence data to determine the possible multipolarities of experimentally observed transitions. The following anisotropy ratio was used for each γ transition:

$$R_{\mathrm{DCO}}=\frac{I(\gamma_1 \text{ at } 153^\circ, \text{ gated with } \gamma_2 \text{ at } 99^\circ)}{I(\gamma_1 \text{ at } 99^\circ, \text{ gated with } \gamma_2 \text{ at } 153^\circ)}. \quad (1)$$

These ratios were calibrated for transitions with known multipolarities and spin sequences. For the placement of lines with weaker intensities such as those that appear above the 28-ns isomer [3], summed DCO spectra were used over γ's of the same multipolarity to enhance the intensities and facilitate comparison. The acceptance window was then determined to be $0.8\leqslant R_{\mathrm{DCO}}\leqslant1.20$ when comparing against a known dipole with the lower limit for the mixed $E2$-$M1$ transitions, the upper limit for the possible j-j transitions and a typical ratio of 1.0 indicated a dipole. A stretched quadrupole transition is expected to have a $R_{\mathrm{DCO}}\sim0.6$. For most transitions, the energy systematics as well as the existence of parallel low-energy radiations further corroborates the spin assignments suggested by the DCO ratios with the underlying assumption that spin increases monotonically with excitation energy along the most intense pathways. Finally, it was seen that there was a high degree of contamination from neighboring nuclei, in particular ^{150}Dy, indicating that some

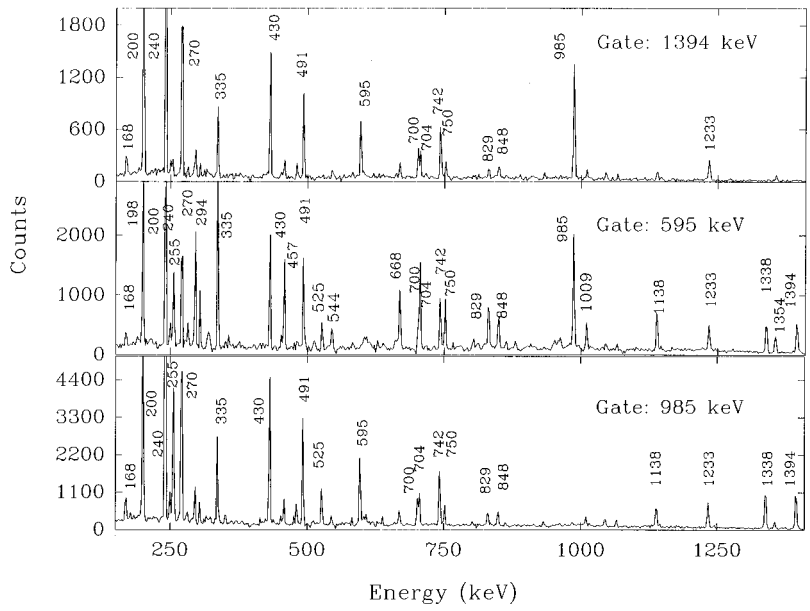

FIG. 2. Coincidence spectra with gates on the 985 keV, 595 keV, and 1394 keV transitions.

of these lines were ''shared.'' In these cases intensity arguments alone were not reliable in placing such lines and another method was used. For example, in the region of the transition energy of 199 keV we see three transitions: 197.7 keV, 199.6 keV, and 200.1 keV. We were able to isolate two of these transitions (197.7 keV and 199.6 keV) and place them as shown in Fig. 1. This was done by first gating on the 1354 keV transition in which the 197.7 keV line is more intense than the 199.6 keV line. Furthermore, upon overlaying the 1354 keV gate with the projected spectra of the 849 keV, 704 keV, 750 keV, and 1009 keV γ rays it was seen that the 197.7 keV transition was not in coincidence with these individual gates. Using similar arguments, it was not possible to unambiguously ascribe the 200.1 keV γ ray to the nucleus ^{149}Dy. The 985-keV, 253-keV, and 270-keV lines are good examples of ''doublets'' and only one of each of these has been placed with certainty. We believe that the level structure established in this experiment is unambiguous with the spins and parities indicated. Uncertain assignments are enclosed in parentheses in keeping with the convention.

III. THEORY

The bulk properties of the experimental level scheme indicate a spherical nucleus. Theoretical calculations were carried out using a nuclear Hamiltonian represented by a Woods-Saxon mean-field potential and assuming a monopole pairing force as a short-range residual interaction [8,9]. The results were consistent with the findings of Möller *et al.* [10], who predict a very slightly oblate equilibrium deformation ($\beta_2 = -0.044$) for ^{149}Dy. In order to facilitate the assignment of shell-model configurations to each level, a more detailed phenomenological (but microscopic) calculation was carried out. The method utilizes single-particle energies and the nucleon-nucleon interaction energies obtained from the ground-state masses and the experimental excitation energies of ^{146}Gd and its $N=82,83$ neighbors. The technique is parameter independent and was proposed by Garvey and Kelson [11,12] for ground-state masses based on the prescription by Talmi and de Shalit [13,14]. The method was later extended to include excited states by Blomqvist and collaborators [15], providing the framework that we have successfully used here. The approach restricts the analysis to states that predominantly contain a single configuration as may be expected of most yrast levels.

The assignment of the shell-model configurations to high-spin states such as the $(35^+/2)\hbar$, $(37^+/2)\hbar$, $(39^+/2)\hbar$. and $(41^+/2)\hbar$ levels has been done earlier [16]. These states have been found to be multiplets described by $\pi(h^3_{11/2}d^{-1}_{5/2})\nu f_{7/2}$ and $\pi(h^3_{11/2}\ g^{-1}_{7/2})\nu f_{7/2}$. In order to establish the accuracy of this alternate approach, we have as a first step calculated the energy of the maximally aligned $(41^+/2)\hbar$ state given by $\pi(h^3_{11/2}g^{-1}_{7/2})\nu f_{7/2}$. While following the prescription used in [15] this configuration was broken down into smaller constituent substructures, each of which corresponds to a specific level in a particular neighboring nucleus. We have used two sets of substructures to calculate the energy at the $(41/2)^+\hbar$ state: the first set (set 1) is given by $(\pi h^3_{11/2}g^{-1}_{7/2})$ from ^{148}Dy, $(\pi h_{11/2}\nu f_{7/2})$ from ^{148}Tb, $(\pi g^{-1}_{7/2}\nu f_{7/2})$ from ^{146}Eu, $(\pi h_{11/2})$ from ^{147}Tb, $(\nu f_{7/2})$ from ^{147}Gd, and $(\pi g^{-1}_{7/2})$ from ^{145}Eu. The specific calculation for $E_{41/2^+}$ using this set is

$$
\begin{aligned}
E_{41/2^+}[\pi(h^3_{11/2}g^{-1}_{7/2})\nu f_{7/2}] = {} & E_{17^-}(^{148}\mathrm{Dy}) \\
& + 3\times 0.6569 E_{9^+}(^{148}\mathrm{Tb}) \\
& + 3\times 0.2917 E_{8^+}(^{148}\mathrm{Tb}) \\
& + 3\times 0.05144 E_{7^+}(^{148}\mathrm{Tb}) \\
& - 3\times E_{11/2^-}(^{147}\mathrm{Tb}) \\
& + E_{7^-}(^{146}\mathrm{Eu}) \\
& - E_{7/2^+}(^{145}\mathrm{Eu}) + \mathcal{S},
\end{aligned}
$$

where the fractional numbers denote the recoupling coefficients and the value $\mathcal{S}$ in terms of the binding energies (E_{BE}) specific to these nuclei is

TABLE I. Transition energy (E_γ), excitation energy (E_x), intensity (I_γ, with respect to the 985-keV transition), DCO ratios (R_{DCO}), and the decay from an intial spin parity (I_i^π) to the final spin parity (I_f^π) for the transitions placed in the decay scheme of ^{149}Dy.

E_γ (keV)	E_x (keV)	I_γ (%)	R_{DCO}	$I_i^\pi \rightarrow I_f^\pi$
80.0[a]	7492.0			$45/2^- \rightarrow 43/2^+$
111.0[b]	2661.7			$27/2^- \rightarrow 21/2^+$
168.1	7412.0	3.4±0.3	1.00±0.06	$43/2^+ \rightarrow 41/2^+$
197.7	10763.4	3.5±0.4	0.84±0.07	$(55/2) \rightarrow (53/2)$
199.6	4086.1	33.0±2.0	1.08±0.04	$33/2^+ \rightarrow 31/2^+$
213.0	6893.1			
239.8	3886.5	78.0±5.0	0.98±0.03	$31/2^+ \rightarrow 29/2^+$
253.3	7412.6	5.0±1.0	0.84±0.08	$43/2^+ \rightarrow 41/2^+$
254.9	5479.2	21.0±2.0	0.95±0.04	$37/2^+ \rightarrow 35/2^+$
269.8	5749.0	45.0±3.0	0.94±0.02	$39/2^+ \rightarrow 37/2^+$
294.2	8381.6	8.0±1.0	0.92±0.07	$(49/2) \rightarrow 47/2^-$
299.0[b]	2550.8	80		$21/2^+ \rightarrow 17/2^+$
303.1	11126.2	5.0±1.0	0.88±0.12	
335.1	11098.5	17.0±1.0	0.86±0.05	$(57/2) \rightarrow (55/2)$
350.0	7243.4	1.9±0.4		
430.3	6179.3	44.0±3.0	0.99±0.04	$41/2^+ \rightarrow 39/2^+$
456.5	9211.4	8.0±1.0	0.66±0.11	$(51/2) \rightarrow (49/2)$
479.2	7159.3	4.0±1.0	1.08±0.13	$41/2^+$
491.1	7413.1	33.0±2.0	1.00±0.04	$43/2^+ \rightarrow 41/2^+$
525.4	5749.6	13.0±1.0	0.94±0.11	$39/2^+ \rightarrow 35/2^+$
543.7	10763.7	4.0±1.0	1.67±0.21	
580.8	6330.4	3.0±1.0		
595.4	8087.4	28.0±2.0	1.17±0.05	$47/2^- \rightarrow 45/2^+$
603.1	10823.1			
667.5	8754.9	7.0±1.0	1.16±0.15	$(49/2) \rightarrow 47/2^-$
700.3	6179.3	10.0±2.0	1.06±0.09	$41/2^+ \rightarrow 37/2^+$
704.2	9915.6	10.0±1.0	1.19±0.08	
742.1	6922.0	23.2±2.0	1.20±0.05	$41/2^+ \rightarrow 41/2^+$
750.4	9961.8	9.0±1.0	1.28±0.14	$(53/2) \rightarrow (51/2)$
802.0	10763.8			
829.3	9210.9	5.0±1.0	1.60±0.24	$(51/2) \rightarrow (49/2)$
848.2	10764.0	5.0±1.0		
861.0	10822.8			
930.5	6680.1	3.0±1.0	1.17±0.33	
984.9	3646.7	100.0±2.0	0.96±0.03	$29/2^+ \rightarrow 27/2^-$
1008.6	10220.0	5.0±1.0	1.07±0.17	
1064.1	7243.4	6.0±1.0	0.67±0.33	$41/2^+ \rightarrow 41/2^+$
1073.0[b]	1073.0	100.0		$13/2^+ \rightarrow 7/2^-$
1138.2	5224.7	15.0±2.0	0.89±0.09	$35/2^+ \rightarrow 33/2^+$
1143.6	12242.1	3.0±1.0	1.50±0.38	$(61/2) \rightarrow (57/2)$
1178.8[b]	2251.8	95.0		$17/2^+ \rightarrow 13/2^+$
1232.5	7412.0	18.0±2.0	1.18±0.07	$43/2^+ \rightarrow 41/2^+$
1337.7	5224.2	45.0±3.0	0.89±0.06	$35/2^+ \rightarrow 31/2^+$
1353.3	10565.7	6.0±2.0	0.90±0.26	$(53/2) \rightarrow (51/2)$
1393.5	5479.6	41.0±3.0	1.80±0.06	$37/2^+ \rightarrow 33/2^+$
1408.9	7185.5	0.7±0.2		$41/2^+ \rightarrow 39/2^+$
1584.0[b]	1584.0			$(11/2^-) \rightarrow 7/2^-$

[a]Assuming that $E_\delta \sim 80.0$ keV, based on the assumptions made in the text. The computation of E_x above this level assumes the energy to be 80.0 keV.

[b]Indicates levels below the 510 ms isomer. The relative intensities of the 111.0, 299.0, 1073.0, and 1178.8 keV transitions have been adopted from Refs. [5,6].

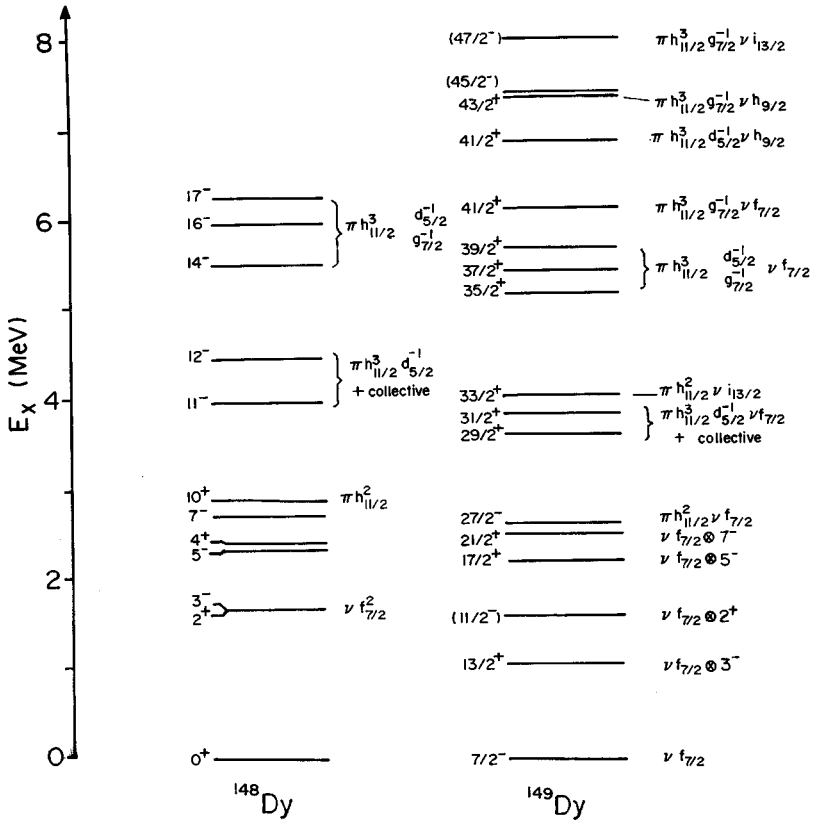

FIG. 3. Assigned shell-model configurations for states in ^{149}Dy when compared against ^{148}Dy.

$$\mathcal{S}=E_{\rm BE}(^{148}{\rm Dy})+3\times E_{\rm BE}(^{148}{\rm Tb})-3\times E_{\rm BE}(^{147}{\rm Tb})$$
$$-3\times E_{\rm BE}(^{147}{\rm Gd})+3\times E_{\rm BE}(^{146}{\rm Gd})+E_{\rm BE}(^{146}{\rm Eu})$$
$$-E_{\rm BE}(^{145}{\rm Eu})-E_{\rm BE}(^{149}{\rm Dy}).$$

The value of $\mathcal{S}$ has been calculated from the ground-state masses and $E_{\rm BE}$ from Refs. [15,17]. Using this procedure, the calculated energy $E_{41/2^+}=6182$ keV with set 1. The second set of substructures used was $(\pi h^3_{11/2}\nu f_{7/2})$ from ^{150}Ho, $(\pi h^3_{11/2}g^{-1}_{7/2})$ from ^{148}Dy, $(\pi g^{-1}_{7/2}\nu f_{7/2})$ from ^{146}Eu, $(\pi h^3_{11/2})$ from ^{149}Ho, $(\nu f_{7/2})$ from ^{147}Gd, and $(\pi g^{-1}_{7/2})$ from ^{145}Eu, corresponding to

$$E_{41/2^+}[\pi(h^3_{11/2}g^{-1}_{7/2})\nu f_{7/2}]=E_{17^+}(^{150}{\rm Ho})+E_{17^-}(^{148}{\rm Dy})$$
$$+E_{7^-}(^{146}{\rm Eu})$$
$$-E_{27/2^-}(^{149}{\rm Ho})$$
$$-E_{7/2^+}(^{145}{\rm Eu})$$
$$-E_{7/2^-}(^{147}{\rm Gd})+\mathcal{S},$$

and in terms of $\mathcal{S}$ for the second set,

$$\mathcal{S}=E_{\rm BE}(^{150}{\rm Ho})+E_{\rm BE}(^{148}{\rm Dy})+E_{\rm BE}(^{146}{\rm Eu})-E_{\rm BE}(^{149}{\rm Ho})$$
$$-E_{\rm BE}(^{145}{\rm Eu})-E_{\rm BE}(^{147}{\rm Gd})+E_{\rm BE}(^{146}{\rm Gd})-E_{\rm BE}(^{149}{\rm Dy}).$$

This calculation yielded the theoretical value of $E_{41/2^+}=6248$ keV. Whereas both of these results compare extremely well with the experimental energy of $E_{41/2^+,{\rm expt}}=6178$ keV, the computation using the first set of substructures is in closer agreement. Following the same procedure and adopting the components of set 1, the theoretical energy for the maximally aligned state at $(43/2^+)\hbar$ described by $\pi(h^3_{11/2}g^{-1}_{7/2})\nu h_{9/2}$ is 7492 keV, in close agreement with the experimental energy of 7410 keV for the same state. We have further calculated the energies of two other $(41/2)^+\hbar$ states with the probable configurations $\pi(h^3_{11/2}d^{-1}_{5/2})\nu h_{9/2}$ and $\pi(h^3_{11/2}g^{-1}_{7/2})\nu h_{9/2}$. The theoretical values were found to be 7200 keV and 7500 keV for the two levels, respectively, in comparison to the corresponding experimental energies of 6922 keV and 7243 keV. Whereas some agreement exists, a closer correspondence between theory and experiment is precluded on account of the closeness in energy of the two levels ($\delta E\sim 300$ keV) and thus the large amount of configuration mixing involved. Finally, the $(47/2^-)\hbar$ state that decays via the 595-keV transition is in all likelihood the maximally aligned $\pi(h^3_{11/2}g^{-1}_{7/2})\nu i_{13/2}$ level. Detailed theoretical computations for this state were not possible owing to the unavailability of data for a pure $i_{13/2}$ state. This was because the mixing between the $\nu f_{7/2}\otimes 3^-$ and the $i_{13/2}$ states was very large in the neighboring nuclei that provided the data for this calculation. It has been noted [18], however, that the estimated *difference* between the single-particle energies at $i_{13/2}$ (2.1 MeV) and $h_{9/2}$ (1.4 MeV) is of the order of 700 keV. This is consistent with our observation wherein the energy difference between the $(47/2^-)\hbar$ level and the $(43/2^+)\hbar$ is of the same order of magnitude. The shell-model assignments based on this study are shown in Fig. 3 in comparison to ^{148}Dy.

IV. RESULTS AND DISCUSSION

It is clear that the decay scheme follows the pattern of levels feeding into maximally aligned configurations. The mechanics of such a scheme are well understood in the context of the shell model as described above. The first such configuration occurs at a spin of $(27/2^-)\hbar$ with the presence of a long-lived isomer $\sim$510 ms, which is highly unusual at such a low energy in the $N=83$ region. We will discuss the scheme in detail, going upward from the ground state. We have placed the new 1584 keV transition feeding into the ground state from the 1584-keV level with a configuration of $\nu f_{7/2}\otimes 2^+$ as assigned by Menegazzo *et al.* [19]. We have confirmed the earlier shell-model configurations assigned to the four levels [6,19] formed by the cascade 1073-1179-299-111. The optimal configuration at the $(27/2^-)\hbar$ state corresponds to the $\nu f_{7/2}$ coupled to the $10^+\hbar$ state in ^{148}Dy as shown in Fig. 3. This $10^+\hbar$ isomeric state is the aligned $\pi h^2_{11/2}$ state with the other members of the multiplet also identified [5]. Up to this point in the scheme, most of the angular momentum is generated by the valence protons. The $(29/2^+)\hbar$ and $(31/2^+)\hbar$ states are quite certainly based upon the 11^- and 12^- states in ^{148}Dy coupled with one neutron in the $f_{7/2}$ state outside the ^{146}Gd core. An assignment of $\pi h^2_{11/2}\nu i_{13/2}$ for the $(33/2^+)\hbar$ state as done in [16] is worth noting. As mentioned earlier and due to the unavailability of experimental data for a pure $\nu i_{13/2}$ state, the exact calculation for any state for ^{149}Dy involving this neutron configuration was not possible. Nevertheless, using the estimate of 2.1 MeV (independently determined by Lach *et al.* [17]) for the energy of the single-particle $\nu i_{13/2}$ state, we have calculated the energy for the $\pi h^2_{11/2}\nu i_{13/2}$ configuration within the context of the alternate shell-model approach. The theoretical energy is $E_{33/2^+}=4382$ keV, in comparison to the experimental value of 4086 keV. Above this level higher angular momentum states are generated by the excitation of a core nucleon. As evidence for core breaking, two effects are commonly seen to occur: first, a larger energy gap (of about 1 MeV in the present case) appears between this and the next level, and second, multiple parallel cascades appear corresponding to the many different ways by which angular momentum may be built. The proton core is ''softer'' in comparison to the neutron core, which is ''magic'' at $N=82$. In order to excite one neutron from the core, an energy corresponding to several MeV is indicated, a requirement that exceeds by far the $\sim$1 MeV gap that is observed here. Using similar arguments, there is every indication that the proton core is broken first, the energy requirements for this being closer to 1 MeV. Also, up to this point in the scheme all of the valence proton states have been ''used up'' so that the states that exist above the $(27/2^-)\hbar$ state must arise as a consequence of breaking the proton core. Additionally, all the nucleons tend to align along a common axis forming multiplets [20] corresponding to the various modes of deexcitation. These multiplets have positive parity and we have assigned to them shell-model configurations as shown in Fig. 3, based on calculations done within the theoretical framework described earlier. It is interesting to note that the most favored configurations up to an excitation energy of 6 MeV in even Dy isotopes are based on the $\pi h^3_{11/2}d^{-1}_{5/2}$ that form multiplets as seen in all the neighboring Dy isotopes [1,5,16,18]. The shell-model configurations for the $(35/2^+)\hbar$, $(37/2^+)\hbar$, and $(39/2^+)\hbar$ levels have already been assigned in [16]. At this point, the $(43/2^+)\hbar$ state deserves special mention. The isomeric state observed at an excitation energy of about 7400 keV can only be explained in the presence of an unobserved low-energy transition above the $(43/2^+)\hbar$ state, of the order of 40 keV$\leqslant E_\delta \leqslant$80 keV, where the upper limit has been suggested earlier [6]. In order to support an attenuation factor of a few nanoseconds, Weisskopf estimates favor $E1$ over $M1$ transitions given that electric dipoles are generally very much more hindered [21]. Since all of the four transitions that depopulate the $(43/2^+)\hbar$ state have been experimentally determined to be $M1$ in nature, we believe that it is quite reasonable to assume that the isomeric state lies directly above this level with a spin-parity assignment of $(45/2^-)\hbar$. Whereas low-energy transitions below 92 keV have been observed in this experiment, it has not been possible to uniquely place these lines in the present scheme. Although the structure of the states above the 28 ns isomeric level seems to be quite independent of the ordering below, it is evidently still single particle in nature. A comparison with the level scheme of ^{150}Dy [1] suggests that (neutron) core breaking may be the primary mechanism occurring in the region above 7400 keV given the presence of the large number of parallel cascades that are visible above the 595 keV transition. Shell-model configurations have not been identified for any of these levels due to large uncertainties regarding deformation and configuration mixing. The spin assignments are tentative and based entirely on the DCO ratios for each transition, although an attenuation in the intensities exists as a consequence of the presence of the isomer.

V. CONCLUSIONS

As a consequence of this experiment, the level scheme for the nucleus ^{149}Dy has been extended up to spins of $61/2\hbar$ corresponding to an excitation energy of about 12 MeV, although definite spin-parity assignments have only been made up to the spin $\frac{43}{2}\hbar$ state. A total of about 27 extra transitions have been observed and two previously placed transitions (451.7 keV and 248.4 keV) around an excitation energy of 6.0 MeV have been removed from the level scheme since these were found to be contaminants from ^{150}Dy.

As one may expect, the low-lying states in this nucleus as in the other $N=83$ isotones are multiplets based on single-particle states (with prominent octupole contributions) coupled to $N=82$ core phonon energies [5,22]. Proton core breaking occurs around an excitation energy of about 4.0 MeV, corresponding to a spin of about $\frac{33}{2}\hbar$ with the possibility of further core breaking occurring again around an excitation energy of about 8.0 MeV. Potential-energy surface calculations based on the Strutinsky method and the cranking approximation [23] indicate the onset of quadrupole deformations only around $I^\pi=40^+$ in the case of ^{148}Dy and at about $I^\pi=30^+$ for ^{150}Dy. Based on these predictions, we expect such shape changes to occur only above a spin of $\frac{60}{2}\hbar$ and lying at a much higher energy than that which can be reliably studied in this experiment. Single-particle behavior is seen to exist throughout and all the features present in the level scheme may be successfully interpreted in the context

of the shell model with no experimental evidence pointing to the possible onset of collectivity up to spins of about $\frac{61}{2}\hbar$ in concurrence with theory. We have successfully used an alternate shell-model approach to explain the details of the level scheme. The technique relies solely on the experimental data from neighboring nuclei and is parameter independent. As a result of this, the configurations assigned using this method are very reliable.

ACKNOWLEDGMENTS

The authors acknowledge Dr. S. S. Ghugre in helping with the experimental setup and the sorting of the tapes and Dr. Y. K. Agrawal for providing the target. The cooperation of the NSC pelletron staff, R. P. Singh, G. Rodrigues, S. Muralithar, and the ''GDA'' group is much appreciated. One of the authors (M.G.) would like to thank Dr. C. Baktash, Dr. J. D. Garrett, Dr. S. Raman, and Dr. Carl Gross for many useful discussions and comments, as well as Dr. M. Smith, Dr. C. Bingham, and the Joint Institute for Heavy Ion Research, for all the enthusiastic support and encouragement while at Oak Ridge. One other author (S.B.P.) would like to thank the Board of Research in Nuclear Sciences, India for financial assistance. Many useful discussions with Dr. J. A. Sheikh are gratefully acknowledged and we thank H. Jin and Dr. C. S. Unnikrishnan for their help with the figures.

[1] M. A. Deleplanque, J. C. Bacelar, E. M. Beck, R. M. Diamond, F. S. Stephens, J. E. Draper, Th. Dossing, and K. Neergard, Phys. Lett. **195B**, 17 (1987).

[2] B. Haas, H. R. Andrews, O. Hausser, D. Horn, J. F. Sharpey-Schafer, P. Taras, W. Trautmann, D. Ward, T. L. Khoo, and R. K. Smither, Phys. Lett. B **84**, 178 (1979).

[3] B. Haas, H. R. Andrews, O. Hausser, A. J. Ferguson, J. F. Sharpey-Schafer, T. K. Alexander, W. Trautmann, D. Horn, P. Taras, P. Skensved, T. L. Khoo, R. K. Smither, I. Ahmad, C. N. Davis, W. Kutschera, S. Levenson, and C. L. Dors, Nucl. Phys. **A362**, 254 (1981).

[4] A. M. Stefanini, P. J. Daly, P. Kleinheinz, M. R. Maier, and R. Wagner, Nucl. Phys. A **258**, 34 (1976).

[5] P. J. Daly, P. Kleinheinz, R. Broda, S. Lunardi, H. Backe, and J. Blomqvist, Z. Phys. A **298**, 173 (1980).

[6] R. Julin, S. W. Yates, S. Lunardi, F. Soramel-Stanco, P. Kleinheinz, A. Chevallier, J. Chevallier, B. Haas, S. Khazrouni, N. Schulz, H. Graf, and J. Blomqvist, KFA/JFL Annual report, 1982; R. Julin *et al.*, in *Proceedings of the Conference on High Angular Momentum Properties in Nuclei*, Oak Ridge National Laboratory, 1982, edited by N. R. Johnson (Harwood Academic, Chur, Switzerland, 1984), Vol. 1, p. 76.

[7] S. S. Ghugre, S. B. Patel, M. Gupta, R. K. Bhowmik, and J. A. Sheikh, Phys. Rev. C **47**, 87 (1993).

[8] W. Nazarewicz, M. A. Riley, and J. D. Garrett, Nucl. Phys. **A512**, 61 (1990).

[9] R. Bengtsson, J. Dudek, W. Nazarewicz, and P. Olanders, Phys. Scr. **39**, 196 (1989).

[10] P. Möller, J. R. Nix, W. D. Myers, and W. J. Swiatecki, At. Data Nucl. Data Tables **59**, 185 (1995).

[11] G. T. Garvey and T. Kelson, Phys. Rev. Lett. **16**, 197 (1969).

[12] G. T. Garvey, Annu. Rev. Nucl. Sci. **19**, 433 (1969).

[13] I. Talmi, Rev. Mod. Phys. **34**, 704 (1962).

[14] A. de Shalit and I. Talmi, *Nuclear Shell Theory* (Academic, New York, 1963).

[15] J. Blomqvist, Peter Kleinheinz, and P. J. Daly, Z. Phys. A **312**, 27 (1983).

[16] D. Horn, O. Hausser, I. S. Towner, H. R. Andrews, and P. Taras, Phys. Rev. Lett. **50**, 1447 (1983).

[17] M. Lach, P. Kleinheinz, M. Piiparinen, M. Ogawa, S. Lunardi, M. C. Bosca, J. Styczen, and J. Blomqvist, Z. Phys. A **341**, 25 (1991).

[18] D. Horn, I. S. Towner, O. Hausser, D. Ward, H. R. Andrews, M. A. Lone, J. F. Sharpey-Schafer, N. Rud, and P. Taras, Nucl. Phys. **A441**, 344 (1985).

[19] R. Menegazzo, P. Kleinheinz, R. Collatz, H. Guven, J. Styczen, D. Schardt, H. Keller, O. Klepper, G. Walter, A. Huck, G. Marguier, J. Blomqvist, and The ISOLDE Collaboration, Z. Phys. A **349**, 13 (1994).

[20] R. Broda, M. Ogawa, S. Lunardi, M. R. Maier, P. J. Daly, and P. Kleinheinz, Z. Phys. A **285**, 423 (1978).

[21] H. Morinaga and T. Yamazaki, *In-Beam Gamma Ray Spectroscopy* (North-Holland, Amsterdam, 1976).

[22] T. Komppa, R. Komu, M. Kortelahti, J. Muhonen, A. Pakkanen, M. Piiparinen, I. Procházka, and J. Blomqvist, Z. Phys. A. **314**, 33 (1983).

[23] T. R. Werner and J. Dudek, At. Data Nucl. Data Tables **50**, 179 (1992).